Adsorption of hazardous chromium (VI) ions from aqueous solutions using modified sawdust: kinetics, isotherm and thermodynamic modelling

Rupa Chakraborty, Renu Verma, Anupama Asthana, S. Sree Vidya & Ajaya Kumar Singh

Published online: 07 Oct 2019.

Submit your article to this journal ⬈

View related articles ⬈

View Crossmark data ⬈

Taylor & Francis
Taylor & Francis Group

Check for updates

ARTICLE

Adsorption of hazardous chromium (VI) ions from aqueous solutions using modified sawdust: kinetics, isotherm and thermodynamic modelling

Rupa Chakraborty[a], Renu Verma[a], Anupama Asthana[a], S. Sree Vidya[b]
and Ajaya Kumar Singh [iD][a]

[a]Department of Chemistry, Govt. V.Y.T. PG. Autonomous College, Durg, India; [b]Department of Chemistry, Kalyan PG College, Durg, India

ABSTRACT

The presence of chromium in aquatic streams due to the discharge of industrial effluents is of great concern because of its toxic nature. Removal of Cr(VI) ion from wastewater is a necessary task. To enhance the adsorption capacity of sawdust for heavy metals, sawdust was modified with formaldehyde and used for the adsorption of heavy metal Cr(VI). The process of modifying was characterised by Fourier Transform Infrared Spectroscopy (FTIR) and Scanning Electron Microscopy (SEM). The effects of various parameters such as pH, contact time, adsorbent dose and initial metal ion concentration on the adsorption process were investigated. The maximum removal of chromium (VI) was found to be 100% at pH 2.0, initial Cr(VI) concentration of 10 mg/L, and adsorbent dose of 4 g/L. Equilibrium isotherms for the removal of Cr(VI) were analysed by the Langmuir, Freundlich, and Temkin isotherm models and the experimental data were well explained by the Freundlich isotherm model. The maximum adsorption capacity was found to be 8.84 mg/g. Kinetic studies were performed by pseudo-first-order, pseudo-second-order, intraparticle diffusion and Elovich models. The R^2 value of the pseudo-second-order model is higher than other kinetic models. Therefore, the obtained data were the best fit with the pseudo-second-order kinetic model. The thermodynamics indicated that the adsorption process of sawdust for Cr(VI) was endothermic and spontaneous in nature.

1. Introduction

Among the various types of pollution, water pollution is a most dangerous one due to heavy metal ions, dyes, phenols, inorganic anions, humic acid and pesticides, etc., present in it, got from the wastewater stream by industrial activities [1–3]. Industrial wastewater affects the environment and causes various dreadful diseases. Heavy metal ions which are non-biodegradable accumulate in the nature. Chromium can exist at different oxidation states ranging from -4 to +6 and the most stable forms of chromium in the environment are trivalent Cr(III) and hexavalent Cr(VI) species. Toxicity of Cr(III) is low. It is an essential trace

element in the human body. The Cr(III) form is insoluble in water and is easily oxidised while, the Cr(VI) anions are highly soluble and most of the hexavalent compounds are toxic, carcinogenic, teratogenic and mutagenic. The hexavalent chromium compounds are widely used in chromium electroplating, textile dyeing, leather tanning, metal finishing, and wood preservation [4,5]. Many health lesions caused by excessive intake of Cr(VI) are cancer and damages in kidney, liver and gastric disorders [6]. World Health Organization (WHO 2004) and United States Environmental Protection Agency (USEPA 2011) have prescribed the permissible limit of drinking water for Cr(VI) as 0.05 mg dm^{-3} [7].

Various conventional methods used for the removal of chromium include ion-exchange [8], chemical precipitation [9], membrane filtration [10], reverse osmosis [11], and electrocoagulation [12]. But these methods have many drawbacks such as high cost, huge amount of toxic sludge production and its disposal problem, incomplete removal, high energy consumption and it also requires an excess amount of chemicals. Therefore, there is a need to try and remove Cr(VI) ions from wastewater and create a suitable treatment method, which are simple, effective, and eco-friendly with low cost. In comparison with other methods adsorption has been more cheaper and an effective method for the Cr(VI) removal from the wastewaters. Activated carbon and nanoparticles [13] are the extensively used as an adsorbent due to its large surface area, microporous structure and high adsorption capacity, but it is expensive. Therefore, there is need to search for a cheaper and an easily available substitute. Consequently, a large number of potentially low-cost adsorbents available include agro-based material [14], micro-organisms [15], industrial wastes [4], animal waste [16] and seaweed [17], which has been prepared for chromium removal as reported in the literature.

Sawdust is generally obtained by sawmills in large quantities as a solid waste. Which is easily available and the price is very low. It is composed of lignin, cellulose and hemicelluloses. Sawdust contains polyphenolic groups they are binders of heavy metal ions. But, without any activation sawdust have low adsorption capacities. Generally, chemically modified adsorbent enhances the surface area of the adsorbent and exhibits a higher adsorption capacity than the unmodified adsorbent. So, there is a need to the preparation of activated carbon from various cheaper and alternative materials.

The main objective of this work is to develop a suitable and low-cost adsorbent which enhances the adsorption capacity by modifying the adsorbent surface for the removal of Cr (VI) ions. The effect of various parameters i.e. initial Cr(VI) concentration, pH, contact time, and adsorbent dose was investigated. Moreover, adsorption isotherm, kinetics and thermodynamics were studied to determine the Cr(VI) removal from aqueous solutions. The main important point of this research work that the adsorbent is easily available, low cost, sustainable, environmental friendly and highly efficient for metal sorption capacity and which is used for heavy metal pollution control and wastewater treatment.

2. Experimental

2.1. Materials and reagents

All chemicals were of analytical reagent grade and were obtained from Merck, CDH and HIMEDIA. Potassium dichromate ($K_2Cr_2O_7$) was received from HIMEDIA. Hydrochloric acid (HCl), sulphuric acid (H_2SO_4) and Acetone (CH_3COCH_3) were obtained from Merck.

Formaldehyde (HCHO), sodium hydroxide (NaOH) and 1, 5-diphenylcarbazide was purchased from CDH.

2.2. Preparation of adsorbate

Synthetic solution of heavy metal was prepared from potassium dichromate ($K_2Cr_2O_7$), dissolved in distilled water to give a concentration of 1000 ppm. The desired concentration of the standard solution was prepared by dilution of the stock solution. Initial pH of the Cr(VI) solutions was 5.29 before addition of adsorbents.

2.3. Preparation of adsorbent

Locally used wood sawdust from local market (Chhattisgarh, Durg) furniture manufacturers were procured. The sawdust was washed several times with double distilled water and sun dried for 8 h. The dried material was stored for subsequent chemical treatment. Two grams of dried sawdust was treated with 20 mL of 0.2 N H_2SO_4 and 5 mL of 39% HCHO. This sample was kept in an oven at 100°C for 4 h. After modification sawdust was washed with double distilled water to remove free formaldehyde and dried at 60°C. Finally, the prepared adsorbent was stored for further use.

2.4. Characterisation analysis

The Fourier transform infrared spectroscopy analyses (FTIR) of the samples were recorded on a Thermo Nicolet Nexus 670 spectrometer. The FTIR spectra for the functional groups on the surface of the materials were recorded at a resolution of 4 cm^{-1} from 500 to 4000 cm^{-1}. The surface morphology of the adsorbent was obtained by Scanning Electron Microscopy (SEM) (JEOL JSM-6390). The determination of the point of zero charge (pH_{pzc}) of the MSD was carried out to a series of conical flasks, 5 mL of KNO_3 solution (0.1 M) was transferred to each conical flasks and the initial pH (pH_i) of the solution was maintained in between 2.0 and 10.0 by adding 0.1 N HCl or 0.1 N NaOH solutions. 0.1 g of MSD was added to each flask and the suspensions were securely capped and shaken for 24 h on an orbital rotatory shaker at 150 rpm. The final pH (pH_f) of the solution was find out and noted accurately. The difference of initial (pH_i) and final (pH_f) pH values i.e. $\Delta pH = pH_i - pH_f$, was calculated and plotted against the initial pH (pH_i) of the solution. The intersection point of the horizontal line (x-axis) in graph at which $\Delta pH = 0$ is the pH_{pzc}.

2.5. Batch adsorption study

The adsorption experiments of Cr(VI) by modified sawdust (MSD) were determined with batch experiments in a water bath incubator shaker (Tempstar). Batch adsorption experiments were carried out in a 100 mL conical flasks filled with 10 mL solution of Cr(VI). The experiments were carried out by varying the pH of the solution (2.0–8.0), contact time (2–20 min), adsorbent dosage (1–6 g/L) and the concentration of Cr(VI) in the solution (5–50 mg/L). 0.1 N HCl and 0.1 N NaOH were used for pH value adjustment by pH metre (Systronics Digital pH Metre-802). Then, proper amounts of dried sawdust (Fig. 1(b)) were added in the above solution with desired initial pH and contact time to achieve

adsorption equilibrium. The initial concentrations of Cr(VI) were 10 mg/L (Fig. 1(a)). After adsorption, the adsorbents were separated by filter paper and then filtrate of the Cr(VI) (Fig. 1(a)) solutions were determined according to the absorbance at the wavelength of 540 nm by a UV-visible spectrophotometer (Systronics UV-Vis spectrophometer- 117). Percentage removal (R%) of Cr(VI) from synthetic solution with modified sawdust was calculated by using the following equation,

The percentage of the Cr(VI) removal R (%) was calculated by this equation:

$$R(\%) = \frac{C_0 - C_e}{C_0} \times 100 \qquad (1)$$

The amount of Cr(VI) ion adsorbed q_e was calculated using this equation:

$$q_e = \frac{C_0 - C_e}{m} \times v \qquad (2)$$

where C_0 and C_e are the initial and equilibrium concentrations of Cr(VI) ion in the aqueous solution, respectively (in mg/L), m is the mass of adsorbent (g) and v is the volume of the solution (L).

3. Results and discussion

3.1. Characterisation of the adsorbents

3.1.1. Fourier Transform Infrared Spectroscopy (FTIR)

The Fourier Transform Infrared Spectroscopy was carried out to analyse the functional group of the surface of the raw sawdust (R-SD) and MSD in the range of 500 to 4000 cm^{-1}. The FTIR spectrums of R-SD and MSD are shown in Figure 2(a,b), respectively (Table 1). In both spectra the broad absorption band at 3418 cm^{-1} is assigned to the – OH stretching vibrations of cellulose, hemicellulose, and lignin. The peak at 2924 cm^{-1} in R-SD is indicating the presence of – CH$_2$ stretching of phenyl propane. The bands around 1643 and 1505 cm^{-1} in R-SD could be assigned to the carboxylic groups. In case of MSD, the peak at 1736 cm^{-1} which indicates the carbonyl (C = O) stretching vibration and this band was strong due to the attachment of carbonyl group on the surface of sawdust as compared to R-SD which confirmed that carbonyl groups were present due to aldehyde
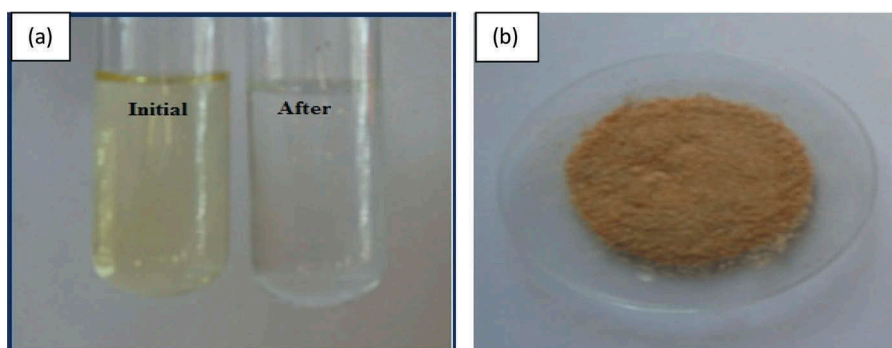

Figure 1. (a) Before and after adsorption of Cr(VI) solution (b) Modified sawdust (MSD).
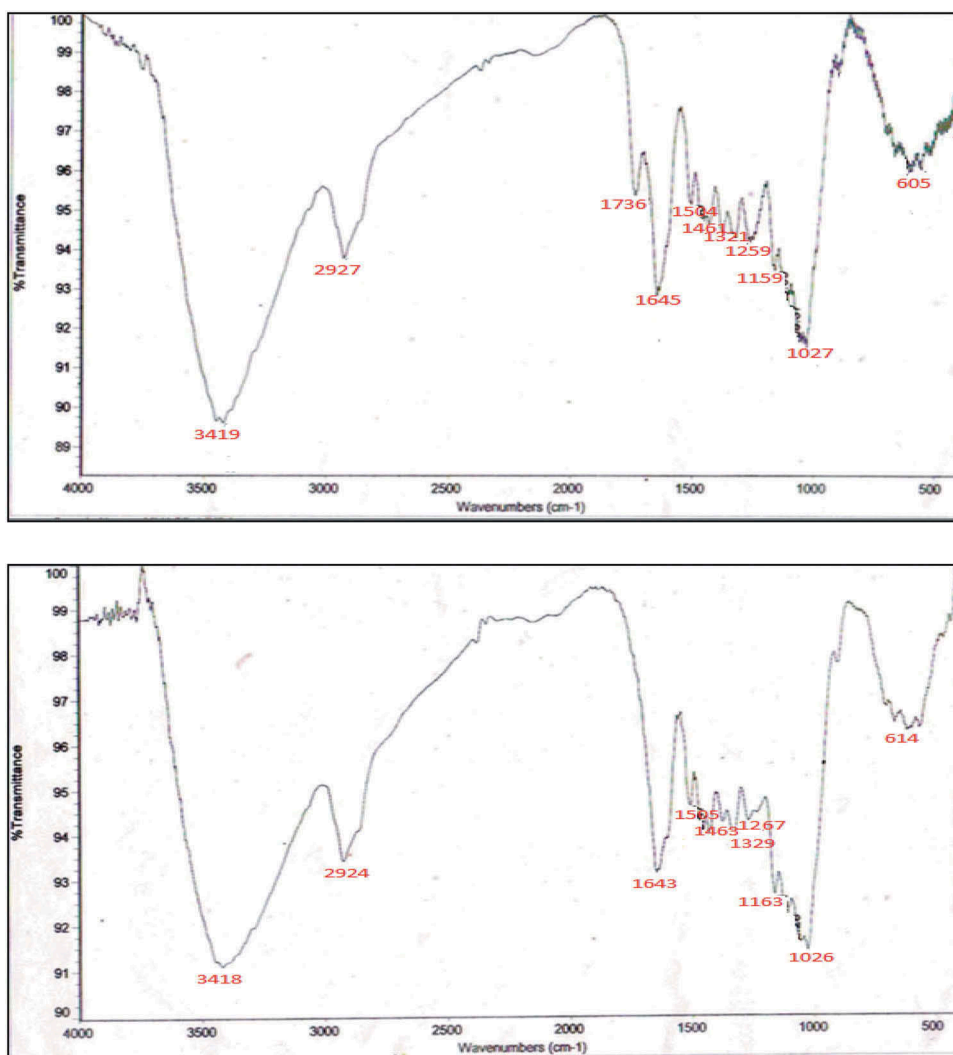
Figure 2. FTIR spectra of (a) R-SD and (b) MSD.

groups attached on the surface of adsorbent after treating it with formaldehyde. The absorption bands at lower wave number range 1463 cm^{-1} and 1461 cm^{-1} were associated with lignin present in sawdust [18] and these peaks are assigned to O-H bending. The peaks in the range 1300–1000 cm^{-1} could be assigned to the C–O stretching vibration of hemicelluloses [19].

3.1.2. SEM characterisation

Scanning Electron Microscopy was used to characterise the surface morphology of the sawdust. Figure 3 indicates the surface morphology of R-SD and MSD at 1000X and 5000X magnifications, respectively. Noteworthy differences were observed between the surface morphology of the R-SD and MSD. As represented in Figure 3(a,b) indicated that the external morphology of R-SD showed much less surface roughness
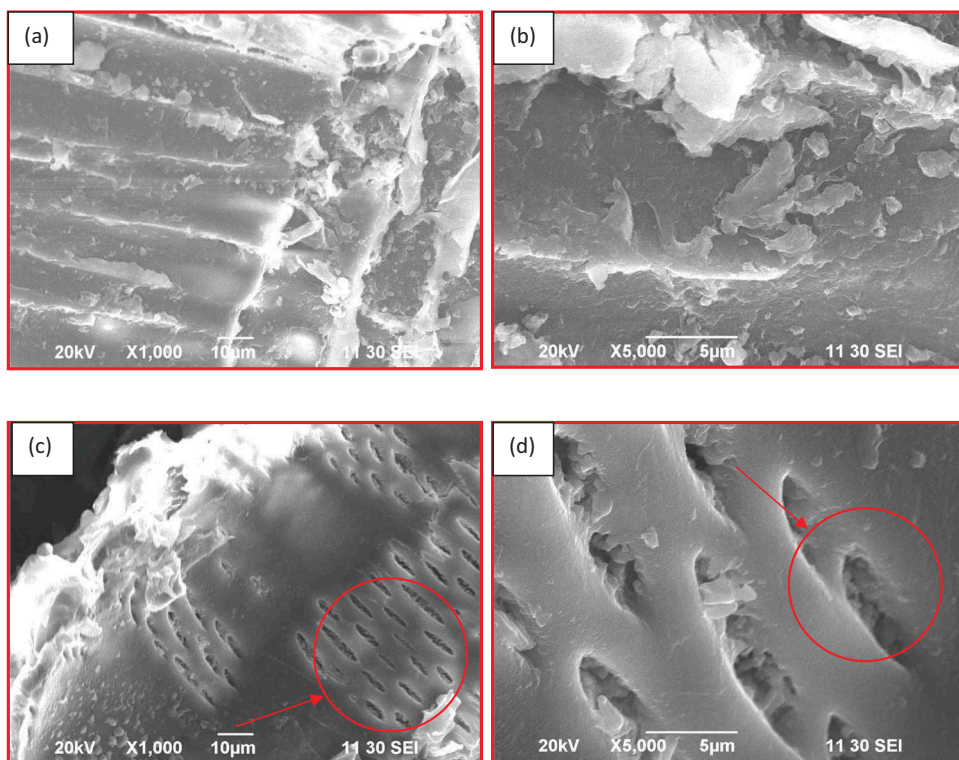
Figure 3. SEM images of (a) R-SD at 1000 magnification, (b) R-SD at 5000 magnification (c) MSD at 1000 magnification, and (d) MSD at 5000 magnification.

morphology (regular plain surface) with no pores on it. Whereas, after modification, the SEM image of MSD in Figure 3(c,d) became rough and ruptured, resulting large cavities (pores) were produced. This indicated high surface area and Cr(VI) ions trapped and adsorbed into these pores.

3.1.3. Point of zero charge

The value of point of zero charge (pH_{pzc}) for MSD was 5.77 (Figure 4). The charges on the surface of the adsorbents depend on this pH_{pzc} value. The MSD surface is positively charged for pH below the PZC (pH < pH_{pzc}), and negatively charged at pH above PZC (pH > pH_{pzc}). According to the literature, chromium present in different oxy-anionic forms such as $HCrO_4^-$, CrO_4^{2-}, $HCr_2O_7^-$, and $Cr_2O_7^{2-}$. The maximum removal of Cr(VI) at acidic pH (pH = 2) and it is below to the pH_{pzc} value (pH < pH_{pzc}). Therefore, it reveals that Cr(VI) adsorption is favourable when the surface of the adsorbent is positive.

3.2. Effect of pH

pH of the solution of chromium is an important parameter which affects the adsorption process. As seen from this figure, the adsorption of chromium (VI) MSD is strongly pH dependent and the removal efficiency decreases continuously
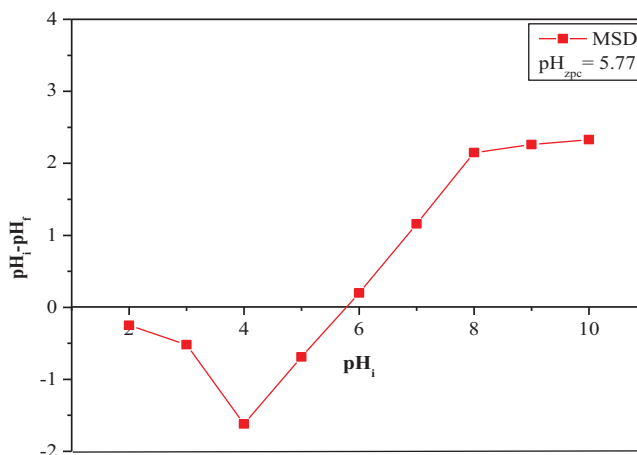
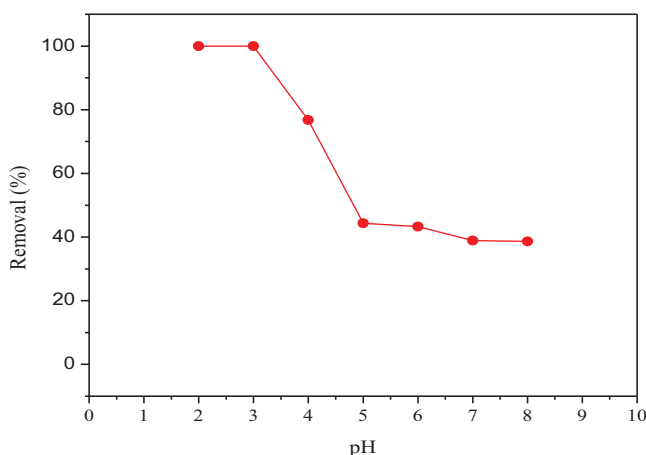**Figure 4.** Point of zero charge (pHpzc) for MSD.

Figure 5. Effect of pH on the removal of Cr(VI) ions using MSD at an initial metal ion concentration 10 mg L^{-1}, contact time 20 min, and adsorbent dose 4 g L^{-1}.

with increase in initial pH from 2 to 8. Chromium removal efficiency was decreased from 100% (at pH 2) to 38.6% (Figure 5). Hexavalent chromium exists in five different forms of H_2CrO_4, CrO_4^{-2}, $Cr_2O_7^{-2}$, $HCrO_4^{-1}$ and $HCr_2O_7^{-}$ in the aqueous solution. $HCrO_4^{-}$ anion is the dominant form of Cr(VI) at a pH 2.0, while CrO_4^{2-} is mostly shown in the range of pH >7. $Cr_2O_7^{2-}$ anions are seen at a pH < 2.0 and H_2CrO_4 exists below a pH < 1.0 [20].

At lower pH, the adsorbent is positively charged due to protonation and dichromate ion exists as anion and the electrostatic forces were developed between them. Thus, the adsorption was high at lower pH and a drastic decrease in adsorption above pH 3. The MSD was analysed using a Fourier Transform Infrared Spectrometer (FTIR) and the result shows the presence of functional groups such as carboxyl and hydroxyl groups responsible for the binding of chromium (VI) onto the surface of MSD. But at a higher pH values the decrease in adsorption may be

due to the overall surface charge on the adsorbents which becomes negative and adsorption decreased.

3.3. Effect of contact time

The effect of contact time on adsorption of Cr(VI) was studied at different times ranged from 2 to 20 min and pH 2. For chromium, minimum percentage removal was 49.4% at time of 2 min and it increased to maximum value 100% at the time of 20 min (Figure 6).

Figure 6 shows that the adsorption rate was fast and adsorption equilibrium reached within 20 min. It can be observed that in the initial stage, the rate of metal uptake on MSD was high because of availability of large number of vacant surface sites for binding with metal ions. As the adsorption increases, the surface of MSD is occupied by Cr(VI) ions gradually, and the rate of removal becomes slower. Then, adsorption reached equilibrium as a result of the reduction of available surface sites which are difficult to be occupied due to electrostatic repulsive forces between adsorbent surface area and the Cr(VI) ions [21–23].

3.4. Effect of adsorbent dose

The dependence of Cr(VI) adsorption on sawdust dose was studied at a room temperature by varying the sawdust amount from 1 to 6 g L^{-1}. Figure 7 shows that the adsorption increased rapidly with increasing adsorbent mass, to a maximum at 4 g L^{-1} for Cr(VI) ion which may be due to greater availability of the vacant sites. After this maximum equilibrium value, the removal efficiency did not increase with increasing adsorbent mass. The percentage of Cr(VI) removal increased from 35.5% to 100% with increasing the MSD dosage from 1.0 to 4.0 g L^{-1}.
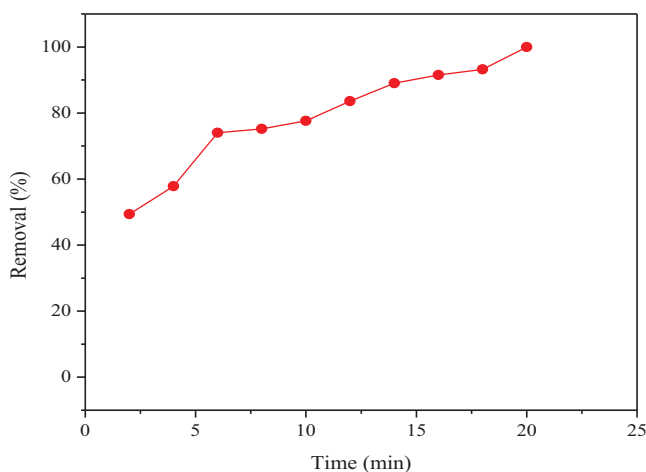

Figure 6. Effect of time on the removal of Cr(VI) ions using MSD at an initial metal ion concentration 10 mg L^{-1}, pH 2, and adsorbent dose 4 g L^{-1}.

Figure 7. Effect of adsorbent dose on the removal of Cr(VI) ions using MSD at an initial metal ion concentration 10 mg L^{-1}, pH 2, and adsorbent dose 4 g L^{-1}.

3.5. Effect of temperature

Effect of temperature on the removal efficiency of Cr(VI) at 20, 30, 40, 45, 50, 55 and 60°C by MSD was studied at an optimum pH of 2.0 and the initial concentration of Cr (VI) was 10 mg L^{-1}. The adsorption efficiency for Cr(VI) increases with the increase in temperature at the range from 20°C to 45°C and remained constant with the rise in temperature (Figure 8). Adsorption is considered as an endothermic process; therefore, increase in temperature increase the adsorption rate [24].
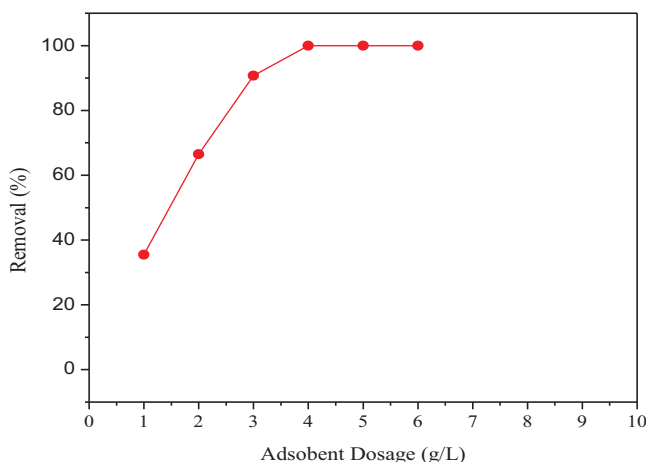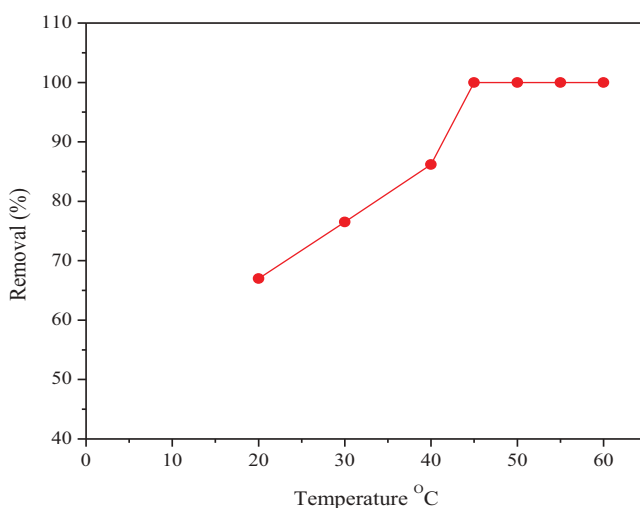

Figure 8. Effect of temperature on the removal of Cr(VI) ions using MSD at an initial metal ion concentration 10 mg L^{-1}, pH 2, and adsorbent dose 4 g L^{-1}.
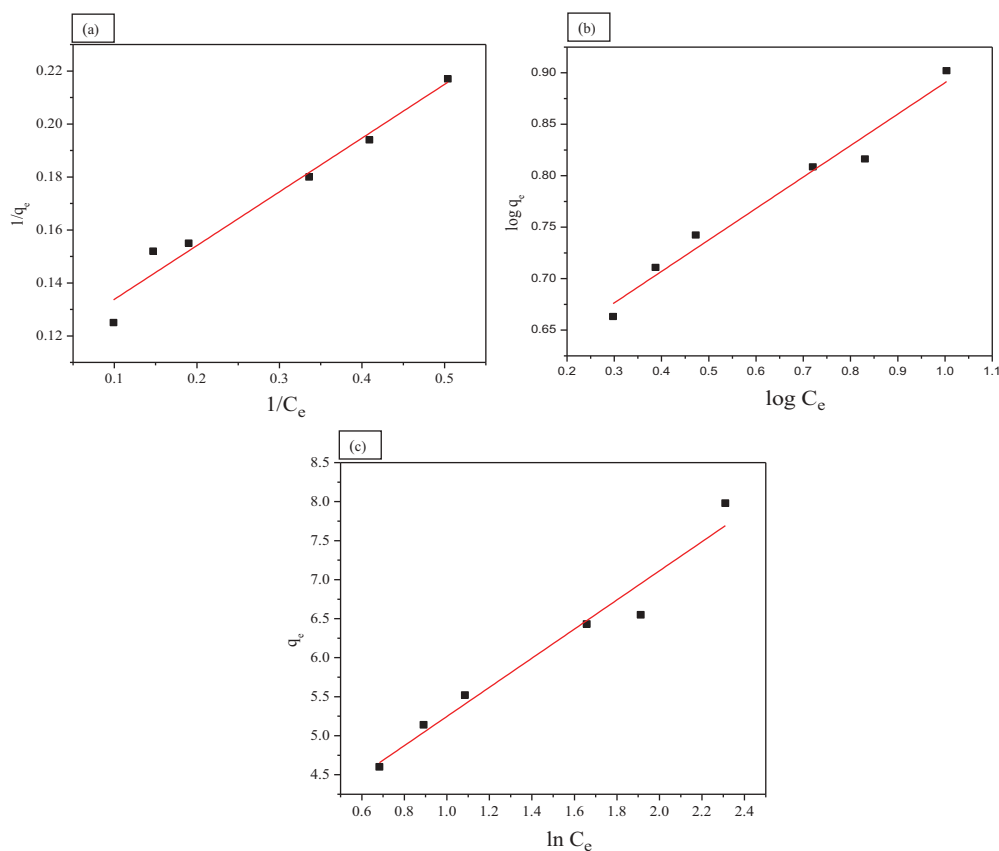
Figure 9. Fit of adsorption isotherms to (a) Langmuir (b) Freundlich (c) Temkin models for Cr(VI) adsorption onto MSD.

3.6. Adsorption isotherm

The conventional adsorption isotherms are used to determine the relationship between the equilibrium adsorption capacity and the equilibrium concentration at a certain temperature. Adsorption isotherms are very useful for determining the adsorption capacity and the interactions between adsorbate and adsorbent [25]. The equilibrium data were fitted to different theoretical models, Langmuir [26], Freundlich [27] and Temkin [28] (Figure 9). Determination of the adsorption mechanism and the correlation coefficient were compared to judge a better fit in order to study the maximum adsorption capacity. The adsorption of Cr(VI) was investigated at room temperature and pH 2.0 with the initial Cr(VI) concentration in the range of 5–50 mg L^{-1}. The Langmuir model is based on the assumption that the adsorption of metal ions occurs on a homogeneous surface by monolayer adsorption without any interaction between the adsorbed ions. The Langmuir equation can be expressed as:

$$q_e = \frac{q_m K_L C_e}{1 + K_L C_e} \tag{3}$$

where q_e is the amount of Cr(VI) adsorbed per specific amount of adsorbent (mg/g), C_e is the equilibrium concentration of Cr(VI) in the solution (mg/L), q_m is the maximum adsorption capacity and K_L is the Langmuir constant (L/mg).

The plots of $1/q_e$ as a function of $1/C_e$ for the adsorption of Chromium were found linear and the values of q_m and K_L was determined by this Equation (4):

$$\frac{1}{q_e} = \frac{1}{q_m} + \left(\frac{1}{q_m \cdot K_L}\right)\left(\frac{1}{C_e}\right) \tag{4}$$

The dimensionless separation factor (R_L), is an essential characteristic of the Langmuir isotherm model. R_L can be determined by the following Equation (5):

$$R_L = \frac{1}{1 + K_L C_0} \tag{5}$$

where C_0 denotes the initial concentration (mg/g). The value of R_L shows the type of the isotherm. The adsorption process is unfavourable at ($R_L > 1$), linear at ($R_L = 1$), favourable at ($0 < R_L < 1$), or irreversible at ($R_L = 0$). The value of R_L is much less than 1, thereby confirming that the adsorption of Cr(VI) onto MSD is a favourable process [29–31].

The Freundlich model assumes that the adsorption of metal ions occurs on a heterogeneous surface by multilayer adsorption. The Freundlich equation can be expressed as:

$$q_e = K_F C_e^{1/n} \tag{6}$$

Equation (6) can be rearranged to obtain a linear form by taking logarithms. The determination of the Freundlich constant is as shown below:

$$\log q_e = \log K_F + \left(\frac{1}{n}\right) \log C_e \tag{7}$$

where q_e is the amount of Cr(VI) adsorbed per specific amount of adsorbent (mg/g), C_e is the equilibrium concentration of Cr(VI) in the solution (mg/L), K_f $(mg/g)(mg/L)^n$ and n are the Freundlich adsorption isotherm constants. The linear plot was found between $\log C_e$ and $\log q_e$ and the values of K_F and $1/n$ can be determined from intercept and slope by Equation (7).

The Temkin isotherm explained the nature of adsorption heterogeneous system. The Temkin isotherm assumes that the adsorption heat linearly decreases with increasing adsorption capacity. The Temkin equation can be expressed as:

$$q_e = B_1 \ln K_T + B_1 \ln C_e \tag{8}$$

where $B_1 = RT/b$, T is the absolute temperature (K) and R is the universal gas constant (8.314 J/mol K). B_1 is the constant related to the heat of adsorption (J/mol), K_T is the equilibrium binding constant (L/g) corresponding to the maximum binding energy.

In this work, the results of the three isotherm equations are listed in Table 2. As Table 2 presented, the R^2 value for the Freundlich isotherm was higher than the other two isotherms, which shows that the Freundlich isotherm was the best fit to the experimental

Table 1. FT-IR spectral characteristics of R-SD and MSD.

IR Peak	R-SD (1/cm)	MSD (1/cm)	Assignment
1	3418	3419	−OH Stretching
2	2924	2927	−CH$_2$ Stretching
3	Absent	1736	C = O Stretching
4	1643	1645	Carboxylic groups
5	1505	1504	Carboxylic groups
6	1463	1461	O−H bending
7	1430	Absent	Symmetric bending of CH$_3$
8	1329	1321	C−O stretching
9	1267	1259	O−H alcohols and aliphatic ether
10	1163	1159	Stretching C−O of COOH
11	1026	1027	C−O Stretching
12	614	605	C−H bending

Table 2. Isotherm model constants and coefficients of determination for adsorption of Cr(VI) onto sawdust.

Adsorbent	Langmuir isotherm				Freundlich isotherm			Temkin isotherm		
	q_m (mg/g)	K_L	R_L	R^2	K_f (mg/g) (mg/L)^n	N	R^2	B_T	K_T (L/mg)	R^2
Sawdust	8.84	0.561	0.151	0.969	3.84	3.27	0.972	1.86	1.81	0.963

data. Thus, it can be concluded that Cr(VI) adsorption onto MSD can be determined for multilayer adsorption processes.

3.7. Adsorption kinetics

The adsorption kinetics indicates the relationship between rates of adsorption with its contact time. The adsorption process was investigated by fitting the experimental data with pseudo-first-order, pseudo-second-order kinetic models and the intra-particle diffusion model.

The pseudo-first-order kinetic model assumes that the adsorption is a pseudo-chemical reaction [32]. The integral form of the pseudo-first-order model is given as:

$$\ln(q_e - q_t) = \ln q_e - k_1 t \tag{9}$$

where q_e and q_t are the adsorption capacity (mg/g) at equilibrium and at time t (time) and k_1 is the rate constant (min^{-1}) of pseudo-first-order adsorption. The values of k_1 and q_e were determined from the slope and intercept of the straight line graph, respectively. The plot of log (q_e-q_t) versus t was shown in Figure 10(a).

The linear form of pseudo-second-order kinetics model is given as:

$$\frac{t}{q_t} = \frac{1}{k_2 q_e^2} + \frac{t}{q_e} \tag{10}$$

where q_e is the amount of adsorbate adsorbed at equilibrium in mg g^{-1}, q_t is the amount of adsorbate adsorbed at time t, in mg g^{-1} and k_2 is the pseudo-second-order rate constant in g mg^{-1} min^{-1}. The linear plot of t/qt versus t was used to determine the values of q_e and pseudo-second rate constant k_2 from the slope and the intercept of the straight line graph, respectively Figure 10(b).

The intra-particle diffusion model is applied to determine the adsorption progress of Cr(VI) by the MSD and it can be represented as:
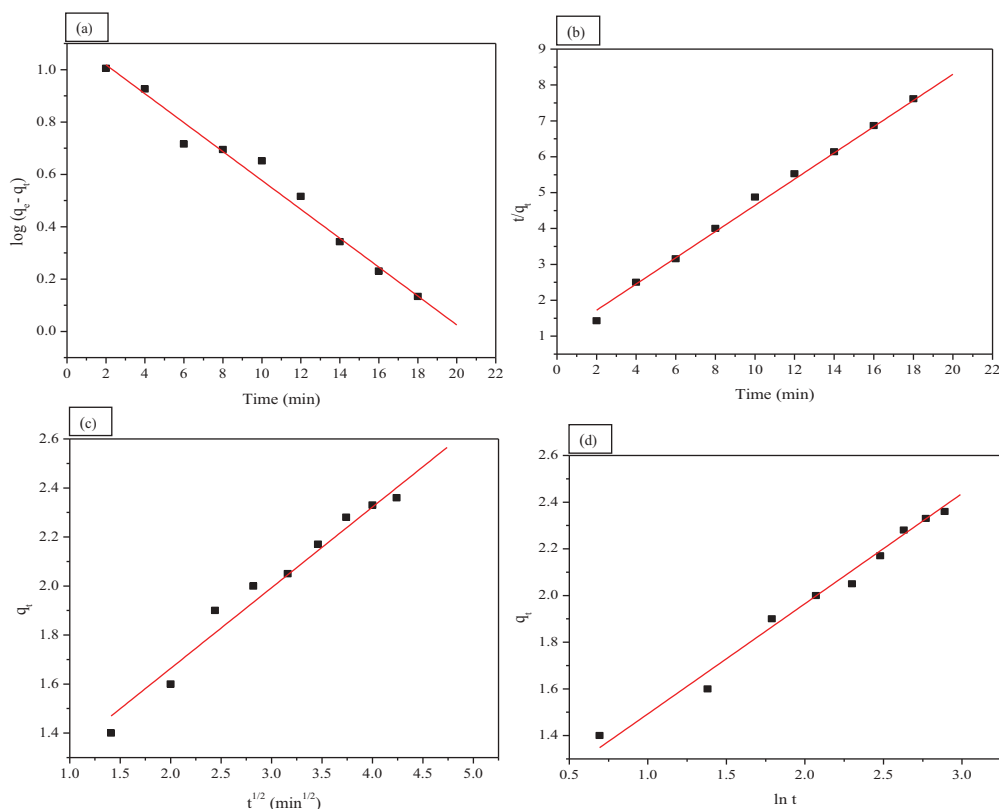
Figure 10. Adsorption kinetics of Cr(VI) ion on MSD (a) pseudo-first order (b) pseudo-second order (c) intraparticle diffusion model and (d) Elovich model at an initial metal ions concentration 10 mg L^{-1}, contact time up to 20 min, adsorbent 4 g L^{-1} and pH 2.

$$q_t = k_{id}t^{1/2} + I \tag{11}$$

where K_{id} shows the intra-particle diffusion model rate constant (mg/g min$^{1/2}$) and I represents the intercept. Value of the intercept I can determine the thickness of molecule boundary layer. The linear plot of q_t against $t^{1/2}$ was used to determine the constants of K_{id} and I were obtained from the slope and intercept, respectively Figure 10(c).

Elovich equation is a rate equation based on a kinetic principle assumes that the adsorption sites increase exponentially with adsorption, which implies a multilayer adsorption [33]. The model is commonly expressed by the following Equation (12):

$$q_t = \frac{1}{\beta}\ln(\alpha\beta) + \frac{1}{\beta}\ln t \tag{12}$$

where α (mg g^{-1} min^{-1}) is the initial adsorption rate and β (gmg^{-1}) is the desorption constant and q_t (mg/g) is the amount of chromium (VI) adsorbed at time t (min) per unit of weight of MSD. The plot of q_t against ln t should yield a linear relationship with a slope of $1/\beta$ and intercept of $(1/\beta)\ln(\alpha\beta)$, which confirms to the Elovich model Figure 10(d).

The parameters and the correlation coefficients (R^2) for the four models are presented in Table 3. This indicates that the R^2 value of the pseudo-second-order model is 0.996,

Table 3. The values of the parameters for different kinetic models fitted to the Cr (VI) adsorption kinetics on sawdust.

C_0 (mg L^{-1})	Pseudo-first- order			Pseudo-second order			Intraparticle diffusion model			Elovich model		
	k_1 min^{-1}	q_e mg/g	R^2	k_2 g mg^{-1} min^{-1}	q_e mg/g	R^2	k_{id} mg/gmin^{-1}	C mg/g	R^2	a mg g^{-1} min^{-2}	B g mg^{-1} min^{-1}	R^2
10	0.124	13.18	0.978	0.158	2.65	0.996	0.344	0.96	0.972	1.04	0.457	0.986

Table 4. Thermodynamic parameters for Cr(VI) adsorption onto sawdust.

C_0 (mg/L)	ΔH^0 (KJ/mol)	ΔS^0 (J/mol/K)	ΔG^0 (KJ/mol)		
			303 K	313 K	318 K
10.0	45.60	162.70	−3.68	−5.42	−6.08

which is higher than that of pseudo-first-order (0.978), Elovich (0.986) and intra-particles diffusion model (0.972). Therefore, the obtained data were the best fit with the pseudo-second-order kinetic model [34–36].

3.8. Adsorption thermodynamics

Thermodynamic parameters indicate the information on the adsorption mechanism and the nature of the adsorption process with respect to Van't Hoff's equation. The changes in Gibbs free energy (ΔG^0), enthalpy (ΔH^0), and entropy (ΔS^0) were obtained using the following equations [37].

$$K_d = \frac{C_A}{C_B} \tag{1}$$

$$\ln K_d = \frac{\Delta S^0}{R} - \frac{\Delta H^0}{RT} \tag{2}$$

The value of ΔG^0 can be determined by Equation (3):

$$\Delta G^0 = -RT \ln K_d \tag{3}$$

where K_d is the thermodynamic equilibrium constant corresponding to the temperatures of 303, 313 and 318 K. C_A and C_B are the concentration on the adsorbate on the adsorbent and residual concentration at equilibrium, respectively. T is the absolute temperature in Kelvin (K) and R is the universal gas constant (8.314×10^{-3} kJ/mol K). The values of ΔS^0 and ΔH^0 were calculated from slope and intercept of van't Hoff plot of $\ln K_d$ versus 1/T shown in Figure 11. The ΔH^0 and ΔS^0 evaluated as 45.60 kJ mol^{-1} and 162.70 Jmol^{-1} K^{-1}, respectively. The positive value of enthalpy indicates the endothermic nature of the process and it shows the possible strong bonding between the metal and adsorbent. The temperature increment with a positive value of ΔS^0 confirmed an increased randomness at the solid–liquid interface during the adsorption process. The value of ΔG^0 was calculated − 3.68, − 5.42 and − 6.08 kJ mol^{-1} for 30°C, 40°C and 45°C, respectively, that Hn MSD was thermodynamically feasible and spontaneous at all temperatures (Table 4). The magnitude of Gibbs free energy change increased with the increasing temperature. The small ΔG^0 (less than − 40 kJ mol^{-1}) indicated that the interaction between adsorbed chromium (VI) and the MSD involved a strong chemical reaction.

3.9. Desorption and Regeneration studies

Chromium adsorbed on the surface of MSD was desorbed using NaOH (10 mL, 1N). For the desorption studies, 0.04 g of MSD was used for the adsorption of 10 mL of 10 ppm Cr(VI) ion aqueous solution at pH 2.0. After the adsorption of MSD, 10 mL
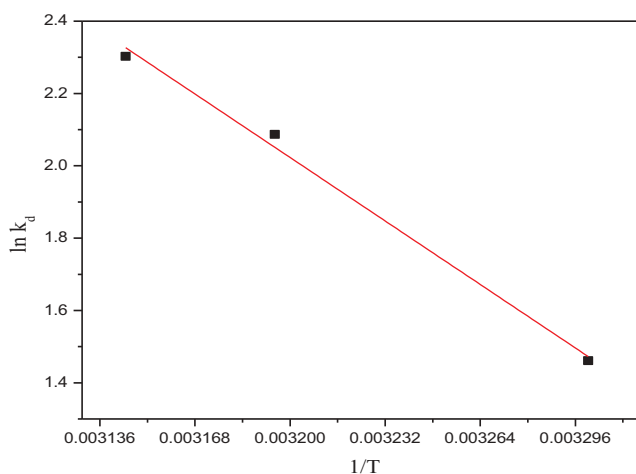
Figure 11. Van't Hoff's plot to determine thermodynamic parameters for removal of Cr(VI) by MSD.

Table 5. Removal of Cr(VI) by various waste materials used as adsorbents and comparison of their maximum adsorption capacity.

S. no.	Adsorbent materials	Adsorption capacity (mg/g)	pH	References
1.	Teff straw	3.51	2.0	[39]
2.	Wheat bran	4.53	2.0	[40]
3.	Modified wheat bran	5.28	2.2	[40]
4.	Walnut shell	8.01	3.5	[41]
5.	Hazelnut shell	8.28	3.5	[41]
6.	Almond shell	3.40	3.2	[41]
7.	Sugarcane bagasse	1.76	2.0	[42]
8.	Rice straw	3.15	2.0	[43]
9.	Rice husk	8.5	2.0	[44]
10.	HCl treated sawdust (H-SD)	6.34	2.0	[45]
11.	Formaldehyde (1%) treated sawdust (HF-SD)	8.2	2.0	[45]
12.	Modified sawdust (MSD)	8.84	2.0	Present work

of 1N NaOH was added in the contents in the conical flask was shaking in an orbital shaking incubator at an rpm of 150. This process was used to determine the reusability of MSD. The adsorption-desorption cycles were repeated for four times.

4. Comparison with other adsorbents for chromium adsorption

Table 5 shows that a maximum Cr(VI) adsorption capacity of various type of adsorbents. The adsorption capacity of MSD was relatively high as compared with other inexpensive adsorbents. Most recently developed materials, such as carbon nanotubes [38] have maximum adsorption capacity for chromium but its cost is expensive, so their use is limited. The waste material (sawdust) used in the present study is generally obtained easily in large amount and its cost is very cheap. Hence, significantly we can conclude that sawdust can be used as a low-cost adsorbent for the removal of chromium.

5. Conclusions

The eco-friendly, low cost and recyclable sawdust were used for effective removal of Cr(VI) ions from the aqueous solution. Modification of sawdust enhanced the adsorption capacity of the MSD due to the increase of carboxylic groups in the adsorbent. The FTIR analysis reveals that the presence of carboxylate groups at the binding site of MSD and the rough surface was found in SEM images. The maximum removal of chromium (VI) was found to be 100% at pH 2.0, initial Cr(VI) concentration of 10 mg/L, and adsorbent dose of 4 g/L. The MSD followed Freundlich isotherm model and pseudo-second order kinetic model. The thermodynamics indicated that the adsorption process of sawdust for Cr(VI) was endothermic and spontaneous in nature.

Disclosure statement

No potential conflict of interest was reported by the authors.

ORCID

Ajaya Kumar Singh ⓘ http://orcid.org/0000-0001-8180-7292

References

[1] E. Derakhshani and A. Naghizadeh, J. Mol. Liq. **259**, 76 (2018). doi:10.1016/j.molliq.2018.03.014.
[2] A. Naghizadeh, M. Kamranifar, A.R. Yari and M.J. Mohammadi, Desalin. Water Treat. **97**, 329 (2017). doi:10.5004/dwt.2017.21687.
[3] M. Ahmaruzzaman and V.K. Gupta, Ind. Eng. Chem. Res. **50**, 13589 (2011). doi:10.1021/ie201477c.
[4] V.K. Gupta, A. Rastogi and A. Nayak, J. Colloid Interface Sci. **342**, 135 (2010). doi:10.1016/j.jcis.2009.09.065.
[5] L. Khezami and R. Capart, J. Hazard. Mater. **123**, 223 (2005). doi:10.1016/j.jhazmat.2005.04.012.
[6] D. Mohan, K.P. Singh and V.K. Singh, Ind. Eng. Chem. Res. **44**, 1027 (2005). doi:10.1021/ie0400898.
[7] K. Huang, Y. Xiu and H. Zhu, Environ. Sci. Pollut. Res. **20**, 5930 (2013). doi:10.1007/s11356-013-1497-0.
[8] S. Rengaraj, C.K. Joo, Y. Kim and J. Yi, J. Hazard. Mater. **102**, 257 (2003). doi:10.1016/S0304-3894(03)00209-7.
[9] M. Uysal and A. Irfan, J. Hazard. Mater. **149**, 482 (2007). doi:10.1016/j.jhazmat.2007.04.019.
[10] C.A. Kozlowski and W. Walkowiak, Water Res. **36**, 4870 (2002). doi:10.1016/S0043-1354(02)00216-6.
[11] C. Li, H. Chen and Z. Li, Proc. Biochem. **39**, 541 (2004). doi:10.1016/S0032-9592(03)00087-6.
[12] A.K. Golder, A.K. Chanda, A.N. Samanta and S. Ray, Sep. Purif. Technol. **76**, 345 (2011). doi:10.1016/j.seppur.2010.11.002.
[13] M. Kamranifar, F. Masoudi, A. Naghizadeh and M. Asri, Desalin. Water Treat. **144**, 233 (2019). doi:10.5004/dwt.2019.23675.
[14] V.S. Mane and P.V.V. Babu, Desalination **273**, 321 (2011). doi:10.1016/j.desal.2011.01.049.
[15] Y. Şahin and A. Öztürk, Process Biochem. **40**, 1895 (2005). doi:10.1016/j.procbio.2004.07.002.

[16] J. Mittal, V. Thakur and A. Mittal, Ecol. Eng. **60**, 249 (2013). doi:10.1016/j.ecoleng.2013.07.025.

[17] V. Murphy, H. Hughes and P. McLoughlin, Chemosphere **70**, 1128 (2008). doi:10.1016/j.chemosphere.2007.08.015.

[18] L. Agouborde and R. Navia, J. Hazard. Mater. **167**, 536 (2009). doi:10.1016/j.jhazmat.2009.01.027.

[19] N. Gierlinger, L. Goswami, M. Schmidt, I. Burgert, C. Coutand, T. Rogge and M. Schwanninger, Biomacromolecules **9**, 2194 (2008). doi:10.1021/bm800300b.

[20] X. Suna, Q. Lib, L. Yang and H. Liu, Particuology **26**, 79 (2016). doi:10.1016/j.partic.2015.11.003.

[21] S. Haider and S.Y. Park, J. Membr. Sci. **328**, 90 (2009). doi:10.1016/j.memsci.2008.11.046.

[22] A.K. Jain, V.K. Gupta and A.B. Suhas, J. Hazard. Mater. **101**, 31 (2003). doi:10.1016/S0304-3894(03)00146-8.

[23] P. Kampalanonwat and P. Supaphol, J. ACS App. Mat. Inter. **2**, 3619 (2010). doi:10.1021/am1008024.

[24] E. Malkoc, Y. Nuhoglu and M. Dundar, J. Hazard. Mater. **138**, 142 (2006). doi:10.1016/j.jhazmat.2006.05.051.

[25] C. Zhou, H. Zhu, Q. Wang, J. Wang, J. Cheng, Y. Guo, X. Zhou and R. Bai, RSC Adv. **7**, 18466 (2017). doi:10.1039/C7RA01147D.

[26] I. Langmuir, J. Am. Chem. Soc. **38**, 2221 (1916). doi:10.1021/ja02268a002.

[27] H. Freundlich, Z. Phys. Chem. **57**, 85 (1906).

[28] M.I. Tempkin and V. Pyzhev, Acta Phys. Chim. Sin. **12**, 327 (1940).

[29] A. Naghizadeh and K. Gholami, J. Water Health **15**, 555 (2017). doi:10.2166/wh.2017.052.

[30] A. Naghizadeh, F. Ghasemi, E. Derakhshani and H. Shahabi, Desalin. Water Treat. **80**, 247 (2017). doi:10.5004/dwt.2017.20891.

[31] B. Adeh, H. Narmin, M. Sadegh, F. Zarei and M. Yazadimamaghani, Iran. J. Chem. Chem. Eng. **36**, 127 (2017).

[32] K. Johari, N. Saman, S.T. Song, H. Mat and D.C. Stuckey, Ind. Eng. Chem. Res. **52**, 15648 (2013). doi:10.1021/ie401470w.

[33] S.Y. Elovich and O.G. Larinov, Assoc. Acad. Doctrine USSR Otd. Khim. Lesson **2**, 209 (1962).

[34] A. Naghizadeh and R. Nabizadeh, Environ. Prot. Eng. **42**, 149 (2016).

[35] M.H. Dehghani, A. Naghizadeh, A. Rashidi and E. Derakhshani, Desalin. Water Treat. **51**, 7655 (2013). doi:10.1080/19443994.2013.791772.

[36] A. Naghizadeh, M. Ghafouri and A. Jafari, Desalin. Water Treat. **70**, 355 (2017). doi:10.5004/dwt.2017.20471.

[37] D. Mohan and K.P. Singh, Water Res. **36**, 2304 (2002). doi:10.1016/S0043-1354(01)00447-X.

[38] M.H. Dehghani, M.M. Taher, A.K. Bajpai, B. Heibati, I. Tyagi, M. Asif, S. Agarwal and V.K. Gupta, Chem. Engg. J. **279**, 344 (2015). doi:10.1016/j.cej.2015.04.151.

[39] B. Tadesse, E. Teju and N. Megersa, Desalin. Water Treat. **56**, 1 (2014). doi:10.1080/19443994.2014.968214.

[40] K. Kaya, E. Pehlivan, C. Schmidt and M. Bahadir, Food Chem. **158**, 112 (2014). doi:10.1016/j.foodchem.2014.02.107.

[41] E. Pehlivan and T. Altun, J. Hazard. Mater. **155**, 378 (2008). doi:10.1016/j.jhazmat.2007.11.071.

[42] I.C. Aloma, I. Rodriguez, M. Calero and G. Blazquez, Desalin. Water Treat. **52**, 5912 (2014). doi:10.1080/19443994.2013.812521.

[43] H. Gao, Y. Liu, G. Zeng, W. Xu, T. Li and W. Xia, J. Hazard. Mater. **150**, 446 (2008). doi:10.1016/j.jhazmat.2007.04.126.

[44] M. Bansal, U. Garg, D. Singh and V.K. Garg, J. Hazard. Mater. **162**, 312 (2009). doi:10.1016/j.jhazmat.2008.05.037.

[45] R. Khalid, Z. Aslam, A. Abbas, W. Ahmad, N. Ramzan and R. Shawabkeh, Chin. J. Chem. Eng. **26**, 614 (2018). doi:10.1016/j.cjche.2017.08.017.